ISSUE: January 2023

Do Eddy Current Effects And Self Heating Cause Distortion In Audio Cables?

by Dennis Feucht, Innovatia Laboratories, Cayo, Belize

Eddy current effects are a fundamental concern in power magnetics design for switched-mode power supply applications. Conceptually, they are a potential concern in another area of electronics—audio applications, specifically in audio cables connecting amplifiers and speakers. Since eddy current effects lead to variations in resistance, they are a potential source of distortion in audio cables. While the issue of audio cable distortion falls outside of the realm of what's typically addressed in power electronics forums, it's notable (and hopefully interesting to designers) that the analytical tools used to design power supply magnetics can also be applied to analyzing audio cable distortion.

However, eddy current effects are not the only source of variation in audio cable resistance. The resistance of a conductor also increases with temperature from self-heating and with the frequency of the current it conducts. An audio cable with resistance R_w in series with resistive load R_L forms a voltage divider. Divider attenuation A_v varies with both time and frequency.

Variation in eddy-current resistance is not an impedance effect and no phase shift occurs. But cable eddy-current inductive reactance also varies with frequency. However, cables are usually designed to have conductors of opposite current polarity in close proximity, and this largely cancels the magnetic fields of each and minimizes inductance. Nevertheless, inductive reactance is present and does vary over the audio frequency range. At 10 kHz, a 1-μH cable has about 63 mΩ of inductive reactance. At 100 Hz, it is 0.63 mΩ, a variation of 2 decades that causes $A_v(j \cdot \omega)$ to vary. Capacitance between opposing conductors also causes $A_v(j \cdot \omega)$ to vary. While inductive reactance and capacitive reactance effects on audio cables are worth considering, they will not be studied in this article.

This article surveys the audio cable analysis problem through magnetics and heat transfer considerations, and includes a magnetics background tutorial on magnetics as it relates to audio cables. Nonlinearity caused by eddy-current effects and self-heating in audio cables is reviewed for audio distortion (IMD and THD) with the bulk of this analysis focusing on eddy-current effects. A tutorial background on the skin and proximity effects in audio cable for determining the extent of cable resistance variation is followed by analysis of a single wire and twisted strands of round wire.

Effects on cable resistance that cause the cable transmittance to be time-variant (such as those due to self heating) cause nonlinearity. After analyzing these effects, we'll consider what improvement in linearity, if any, from plating the periphery of a conductor with a higher-conductivity material such as silver or gold may be achieved.

Skin Effect

The simplest cable to analyze for eddy-current effects is a single (or solid) isolated wire. Without other conducting wires nearby, the proximity effect is absent and only the skin effect occurs. Multi-strand wire has a bundle skin effect.

Fig. 1 shows a conductor cross-section with magnetic field density vector **B** and resulting eddy-currents induced by **B** into the cross-section of the conductor according to Faraday's Law. A magnetic field vector into the page (⊗) induces a CCW current, as shown in Fig. 1. The **B**-field is set up by the main current *i*.

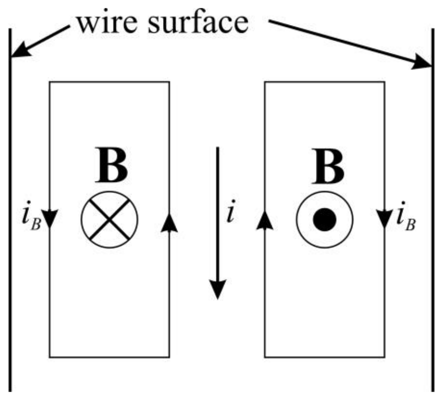

Fig. 1. The skin effect: current i in a wire generates a magnetic field within it that drives the resulting current distribution toward the wire surface. Eddy currents i_B are induced into the conductive wire cross-section by B, canceling i on the inside and aiding it on the outside of their loops.

The inner lines or "filaments" of induced current i_B oppose the main flow i near the center of the wire while near the edges they aid. The effect is an uneven current distribution across the wire whereby most of the current flows at the periphery or "skin" of the wire.

The distribution is graphed in Fig. 2 for a round wire. J is maximum current density, $j(r)$ is the radial current-density distribution, r is the radius from the periphery, and r_c is the conductive radius. The distribution shows an exponential decay from the conductor edge (at 0) to the center (at 1).

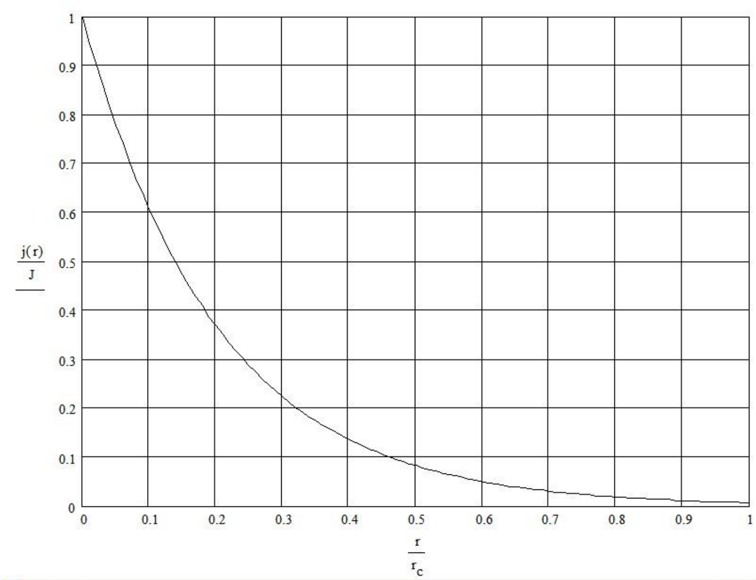

Fig. 2. Graph of current density distribution in the cross-section of a wire. r/r_c = 0 at the wire surface.

Skin depth δ is the width at the conductor edge that the current would flow within if it were uniform in density across δ, as graphed in Fig. 3 for $\delta = 0.2 \cdot r_c$.

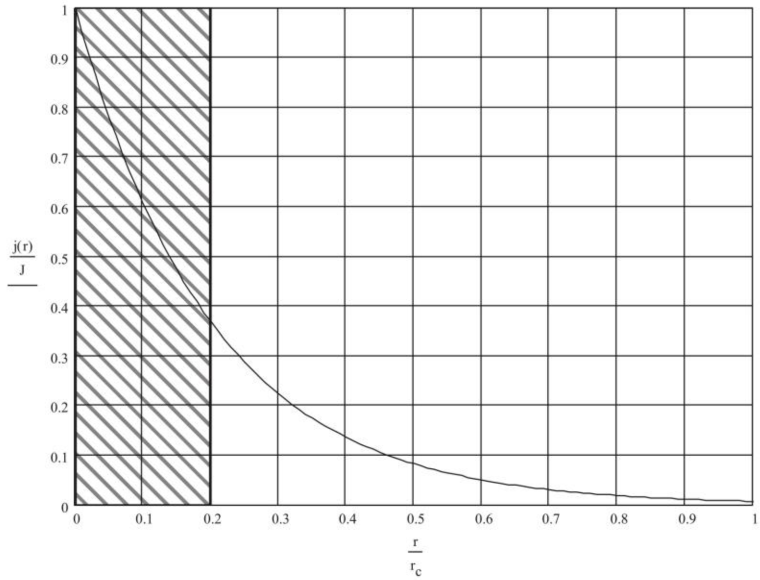

Fig. 3. The equivalent current density from the skin effect has the current flowing uniformly at the wire surface to a depth of δ = 0.2 on this plot.

The area in the hatched rectangle of width δ/r_c is the same as that under the exponential curve;

$$\int_0^{\infty} e^{-r/\delta} \cdot dr = -\delta \cdot e^{-r/\delta} \Big|_0^{\infty} = \delta$$

Thus δ is the depth of the ring from the edge into the wire in which the current would flow were it distributed uniformly within this ring of width δ.

Skin depth is a physical characteristic length or *length-constant* that is derived from fields theory (the Helmholtz diffusion equation) as

$$\delta(f) = \sqrt{\frac{\rho}{\pi \cdot \mu \cdot f}}$$

where ρ is conductor resistivity, μ is permeability, and f is current frequency in Hertz. Besides frequency the other three quantities are either a geometric constant (π) or properties of the conductor material (ρ, μ). They can be lumped together for a given material, resulting in a simplified

$$\delta(f) = \frac{r_\delta}{\sqrt{f/\mathrm{Hz}}} \text{ , 80 °C, } r_\delta(\mathrm{Cu}) = 73.5 \text{ mm, } r_\delta(\mathrm{Al}) = 94 \text{ mm, } r_\delta(\mathrm{Au}) > r_\delta(\mathrm{Cu})$$

Gold has less conductivity than copper and its skin depth is greater. Silver conductivity is more than copper, but not by much.

Wire Size And Resistance Ratios

The skin effect in a round wire of radius r_c is expressed as the round-wire conductor radius in units of skin depth:

$$\xi_r = \frac{r_c}{\delta}$$

If the equivalent of the total current flows at a depth of δ and the wire radius is chosen to be $r_c = \delta$, or $\xi_r = 1$, its conductive area is about 63% at the given frequency of current. Because current distribution is exponential with a tail going to infinity beyond a finite r_c, the utilization is not exactly one; $\xi_r = 1$ is an approximate optimization criterion for isolated (single) wires.

The static-resistance multiplier that accounts for increased resistance from eddy-current effects is F_R. An approximate expression for F_R can be derived for an isolated (single) round wire as the ratio

$$F_{Rw} = \frac{R_w(f)}{R_{w0}} = \frac{\rho \cdot l / A_c(f)}{\rho \cdot l / A_{c0}} = \frac{A_{c0}}{A_c(f)}$$

At 0 Hz, $R_w = R_{w0}$, and the current is uniformly distributed in the wire having an area of

$$A_{c0} = \pi \cdot r_c^2$$

At frequency f the conductor is reduced effectively to that of a ring of thickness δ with cross-sectional area

$$A_c(f) = \pi \cdot r_c^2 - \pi \cdot (r_c - \delta)^2 = 2 \cdot \pi \cdot \left(r_c - \frac{\delta}{2} \right) \cdot \delta = \pi \cdot (2 \cdot r_c \cdot \delta - \delta^2)$$

For physical significance, $\delta \le r_c$ and $\xi_r \ge 1$. Then an approximate

$$F_{Rw} \approx \frac{A_{c0}}{A_c(f)} = \frac{r_c^2}{2 \cdot r_c \cdot \delta - \delta^2} = \frac{\left(\frac{r_c}{\delta}\right)^2}{2 \cdot \left(\frac{r_c}{\delta}\right) - 1} = \frac{\xi_r^2}{2 \cdot \xi_r - 1} \approx \tfrac{1}{2} \cdot \xi_r = \frac{r_c}{2 \cdot \delta} \text{ , } \xi_r >> 1$$
$$F_{Rw} \approx 1, \text{ for } \xi_r < 1$$

The second approximation, of $\xi_r/2$, applies whenever $\xi_r >> 1$. As ξ_r becomes large, the plot of F_{Rw} is asymptotic to a line with a slope of ½. Asymptote $F_{Rw}(\infty)$ is plotted as a dotted line against ξ on the log-log plot in Fig. 4. Some values are also tabulated to the right of the graph.

On the plot,

$$\log F_{Rw} = \log(\xi_r) - \log 2 \text{ , } \xi_r \to \infty$$

The approximated F_{Rw} is minimum for $\xi_r = 1$; $F_{Rw}(1) \approx 1$.

F_{Rw} of an isolated single wire increases with ξ_r as does R_w. As frequency decreases, δ increases monotonically until the resistance is the static resistance. For $\xi_r < 1$, δ exceeds the radius of the wire. The increase in F_{Rw} as given above for $\xi_r < 1$ expands the shell of current beyond the center of the core itself in the approximation but continues to reduce the exact F_{Rw}.

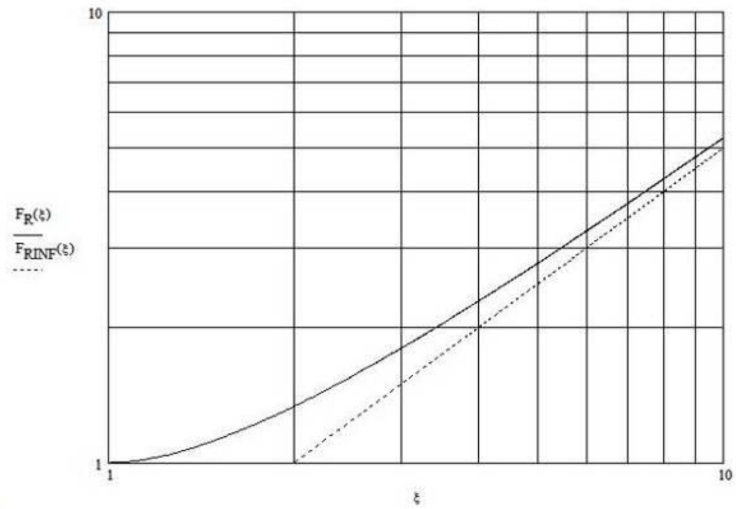

ξ_r	F_{Rw}
1	1
1.5	1.125
2	1.333
2.5	1.563
3	1.800
3.5	2.042
4	2.285
5	2.778
10	5.263

Fig. 4. Graph and table of skin resistance F_R relative to resistance for a constant current as a function of round-wire radius ξ_r in units of skin depth δ. F_{Rw} is the resistance ratio for a single wire isolated from external magnetic fields.

The F_{Rw} equation was derived on the assumption of uniform current in the shell but it actually decreases exponentially toward the center. Because it is not uniform in density as was assumed, the exact F_{Rw} for decreasing ξ_r asymptotically decreases toward one and is the solution of a modified Bessel equation. The current density at the center of a round conductor spans its range from about all to none over the range of about $1 \leq \xi_r \leq 10$.

Strands Of Wire

To demonstrate that a cable consisting of multiple strands of reduced wire size can increase conduction and decrease $R_w(f)$, consider the simple case of comparing a wire of conductive radius r_c and area A_{c1} with two wires, each of area $A_{c2} = A_{c1}/2$ and radius $r_c/\sqrt{2}$. The smaller wires have the same total static conductive area as the larger wire. The effective areas having skin depth δ are, to use the uniform-current-in-shell approximation,

$$A_{c1} = \pi \cdot r_c^2 - \pi \cdot (r_c - \delta)^2 = \pi \cdot (2 \cdot r_c - \delta) \cdot \delta$$

$$A_{c2} = 2 \cdot \pi \cdot \left[\left(\frac{r_c}{\sqrt{2}} \right)^2 - \left(\frac{r_c}{\sqrt{2}} - \delta \right)^2 \right] = 2 \cdot \pi \cdot \delta \cdot \left(\sqrt{2} \cdot r_c - \delta \right)$$

A larger cross-sectional area has lower resistance. To compare, the area ratio is

$$\frac{A_{c2}}{A_{c1}} = \frac{2 \cdot (\sqrt{2} \cdot \xi_r - 1)}{2 \cdot \xi_r - 1}\ , \ \xi_r = r_c / \delta$$

A ratio of greater than one favors the smaller wires. At $f_\delta(r_c)$, $\xi_r = 1$, the ratio is about 0.828, and the larger wire has lower resistance. Crossover is at $\xi_r = 1/2 \cdot (\sqrt{2} - 1) \approx 1/0.828 \approx 1.207$, and $F_{Rw} \approx 1.030$. For increasing ξ_r the smaller wires collectively as a bundle have lower resistance. (A lower limit on resistance for reduced wire size is reached because the conductive area to total bundle area, or *packing factor* $k_p = A_c/A_b$ of the wires, decreases sublinearly with decreasing r_c, and as we will see, from the proximity effect because of an increase in number of strand layers.

Frequency-Dependent Resistance

The ratio of total resistance of a conductor at frequency f to its static (0 Hz) resistance R_{w0} is designated as the *frequency-dependent resistance factor*

$$F_R = \frac{R_w(f)}{R_{w0}}$$

Total resistance, which includes eddy-current effects, is then

$$R_w(f) = F_R \cdot R_{w0}$$

Expressed in *dynamic resistance* $R_{w\sim}$ caused by varying component $i_\sim$ of the current,

$$R_w(f) = R_{w0} + R_{w\sim} = R_{w0} \cdot \left(1 + \frac{R_{w\sim}}{R_{w0}}\right) \Rightarrow$$

$$F_R = \frac{R_w(f)}{R_{w0}} = 1 + \frac{R_{w\sim}}{R_{w0}}$$

For symmetric bipolar waveforms such as sine-waves, F_R applies to the entire waveform. Ohmic power loss of a cable can be expressed in F_R with current waveform *form factor*

$$\kappa = \frac{\tilde{i}}{\bar{i}}\ ,\ \tilde{i} = \text{rms current},\ \bar{i}\ = \text{average current}$$

and waveform *ripple factor*

$$\gamma = \frac{\Delta i/2}{\bar{i}} = \frac{\hat{i}_\sim}{\bar{i}}\ ,\ \hat{i}_\sim\ = \text{ripple amplitude}$$

The RMS current squared, decomposed into its average or static and varying components, is

$$\tilde{i}^2 = \bar{i}^2 + \tilde{i}_\sim^2 = (\kappa \cdot \bar{i})^2$$

Total RMS current is expressed in κ and average current. Then solving for the varying or ripple RMS component,

$$\tilde{i}_\sim = \sqrt{\kappa^2 - 1} \cdot \bar{i}$$

The average winding power loss is

$$\overline{P}_w = R_w \cdot \tilde{i}^2 = (F_R \cdot R_{w0}) \cdot (\kappa^2 \cdot \bar{i}^2) = F_R \cdot \kappa^2 \cdot \overline{P}_{w0}$$

The static power is

$$\overline{P}_{w0} = \bar{i}^2 \cdot R_{w0}$$

Additional loss occurs because of the ripple harmonics. A triangle-wave waveform has a ratio of total electrical power loss to static power loss of

$$\frac{\overline{P}_w}{\overline{P}_{w0}} = F_R \cdot \kappa^2 = F_R \cdot \left[1 + \left(\frac{\gamma^2}{3}\right)\right] \text{, triangle-wave ripple}$$

This indicates how much greater the loss is because of the eddy-current effects. For a constant waveform, $\gamma = 0$.

Proximity Effect

The skin effect is intra-conductor or intra-bundle; the proximity effect is an inter-conductor effect and applies to cables with twisted strands of wire. Wires in close proximity share B-fields and magnetically couple, wire to wire, as shown in Fig. 5. Current *i* flowing downward through the inner wire generates the B-field coming out of the page according to the right-hand rule.

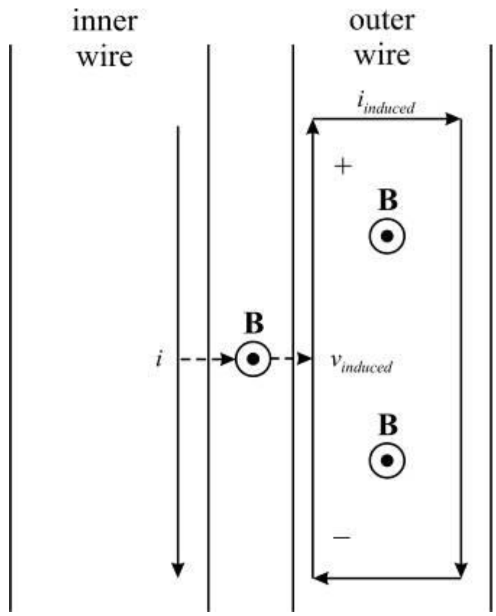

*Fig. 5. The proximity effect is like the skin effect, but from another wire in proximity. The outer wire has induced into it from magnetic field **B** of i in the inner wire a current that crowds its current distribution away from the inner wire. The same happens for the inner wire. Varying currents in proximity to each other repel each other.*

As *i* varies in time, *B* varies and induces a voltage, as shown in Fig. 5, into the adjacent wire linked to **B** according to Faraday's Law:

$$v_{induced} = -\frac{dB}{dt}$$

The induced voltage causes current to flow on the near side of the outer wire in the opposite direction (hence the negative sign in Faraday's Law) to that of the inner wire. On the outer side of the outer wire, current flows in the same direction as *i*. Currents flowing in the same direction in adjacent wires will repel each other and concentrate on the opposite sides of the two wires. If they are of the same winding, then the outer wire has in addition to the induced current the winding current *i*. Its outer side thus supports 2·*i* of current, *i* from the winding current and another *i* from the induced current.

The larger picture for a winding cross-section is shown in Fig. 6. (Rotate the top of Fig. 5 into the page and flip right to left. The left-side inner two conductors are shown in Fig. 6.) Although each winding layer on each side of the loop conducts the same amount *i* of net current, successive outer layers accumulate the mutual coupling effect because the induced current from inner layers adds to *i* to produce additional induced current in the outer layers. The dashed arrows point to the currents they contribute by mutual field coupling. This is the proximity effect.

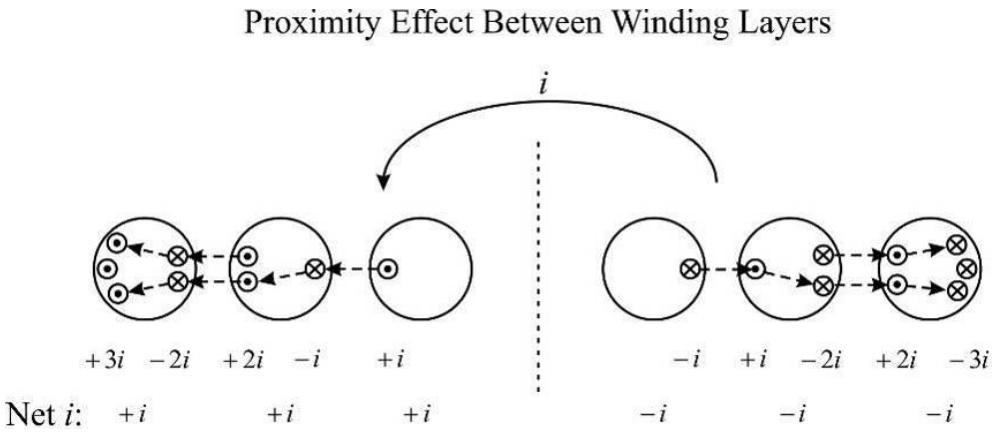

Fig. 6. The proximity effect has a cascading effect on multiple winding layers. Loss from the effect grows worse with layers by M^2 for M = number of layers.

Between layers, **B** points upward. Moving outward, its magnitude *B* increases for each successive layer until, at the outer side of the outermost layer, it is greatest. Applying the simplified form of Ampere's Law,

$$H \cdot l = Ni = M \cdot i \;\Rightarrow\; B = \mu \cdot \frac{M \cdot i}{l}$$

where *l* is the loop length and *M* is the number of layers of current *i* enclosed by a given layer (including its own *i*). The additional induced current dissipates power in the winding along with winding-terminal current *i*. Each successive layer adds more current, and the total current increase over single-layer current *i* for *M* layers is

$$\sum_{m=1}^{M}(m+[m-1]) = 2 \cdot \frac{M \cdot (M+1)}{2} - M = M^2 = 1, 4, 9, 16, \ldots$$

The M^2 rate of increase of the sequence causes an M^4 rate of increase in conductor power loss,

$$P_w = R_w \cdot (M^2 \cdot i)^2 = M^4 \cdot R_w \cdot i^2$$

The proximity effect can be much greater than the skin effect for multiple winding layers and often causes the more inclusive F_R—the sum of both skin-effect $F_R = F_{RS}$ and proximity-effect $F_R = F_{RP}$—to be increased;

$$F_R = F_{RS} + F_{RP}$$

The *B*-field from an adjacent conductor is orthogonal to the *B*-field produced in the conductor from the skin effect, and the two effects combine by algebraic addition. The skin effect produces opposing fields on each side of a layer of wire strands—odd symmetry for **B**—while the proximity effect is caused by the field contribution from other layers, is external to the layer, and of the same polarity on both sides of it—an even symmetry.

The Dowell Eddy-Current Equation

Field derivations have produced formulas for the combined skin and proximity effects. They were originally published by P. J. Dowell in the *Proceedings of the IEE*, August 1966, and are not repeated here. His results are our starting point for including frequency effects in audio cables. With multiple-strand bundles, fields of the turns interact according to the proximity effect.

Dowell's equation is of the form $F_R(\xi, M)$ where ξ is not that of a round wire but of a flat conductive plate. To convert to round wire, a geometric conversion constant,

$$g_r = \sqrt{k_{pw}} \cdot 2 \cdot \left(\frac{\pi}{4}\right)^{3/4} \approx 1.547$$

is included so that $\xi = g_r \cdot \xi_r$. $\xi = \xi(f) = r_c/\delta(f)$. Wire radius r_c can be expressed instead in AWG and held at a fixed wire size while f is swept for a frequency response plot of $F_R(\xi(f), M)$.

The number of layers of N_s strands in a twisted bundle is approximated as though the bundle were square, with $\sqrt{N_s}$ layers and $\sqrt{N_s}$ strands per layer. If the strands form rings around a central strand, the layer count is the same. Then the strand count is the square of the layer count;

$$M = \sqrt{N_s} \Rightarrow N_s = M^2$$

For a given strand wire size, as f varies, ξ is proportional to $f^{1/2}$, and a graph of $F_R(\xi, M)$ against ξ_r as the independent variable and M as parameter results in a family of curves, shown in Fig. 7 on the left. What is more useful for audio analysis is $F_R(f, M)$, shown in Fig. 7 on the right—the frequency response of $F_R(f, M)$ with layers M as parameter.

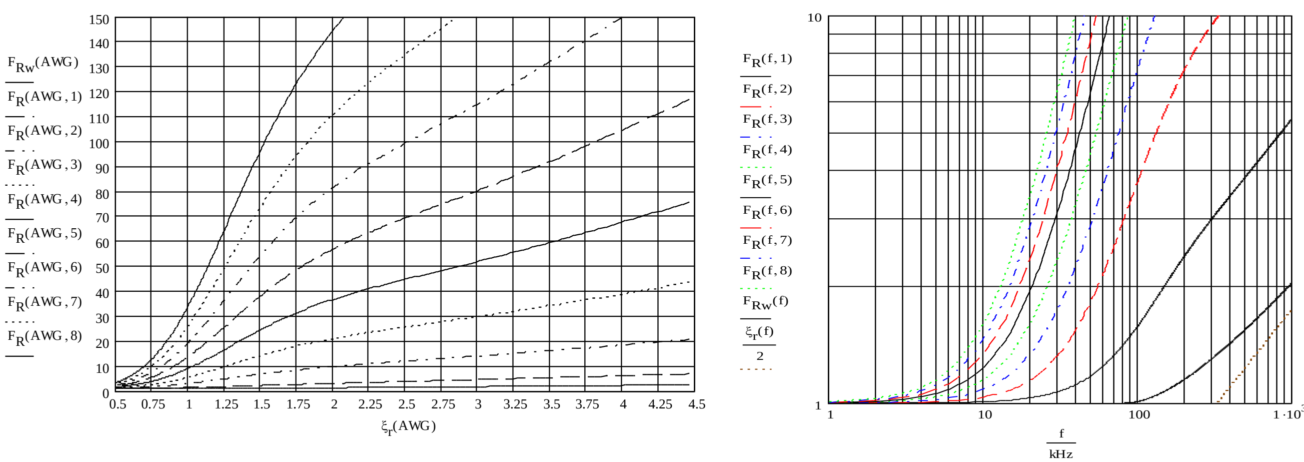

Fig. 7. Graphs of (left) constant wire-radius resistance ratio F_R versus wire radius in units of skin depths ξ_r and (right) $F_R(f, M)$ in frequency f in kHz and for 24 AWG wire. The steeply rising region of the curves is caused by the proximity effect which in multiple layers dominates over the skin effect.

As strand count and thus strand layers M increase, F_R is increased by M^2. A single isolated wire has the lowest $F_R = F_{Rw}$ approximated by $\xi_r/2$ on the Fig. 7 graph. For a single strand, $F_R(f, 1) > F_{Rw}$ because the Dowell equation is based on parallel conductors, and $F_R(f,1) \approx 2 \cdot F_{Rw}$.

The lowest F_R is achieved with many parallel strands of small wire, and the *bundle* F_R for N strands is

$$f_R = \frac{F_R}{N_s}$$

As cable area is held constant and wire size decreases, strand and layer counts increase. The curves become asymptotic with large M in the high-ξr region. Adding strands increases cable strand layers, but the layer curves each have a parallel asymptote. In the low-ξ_r region, the f_R curves flatten below 10 kHz, as they approach 0 Hz. Their quasistatic (0+ Hz) values are minimum and linearly related, decreasing with increasing N_s. Eddy-current effects are minimized by using many strands of small twisted wire.

Eddy-current effects are shown in Fig. 8. The three distinct regions of f_R are distinguished by slope. In the mid-f region of dominant proximity effect, the change in f_R, or Δf_R, is highest, and is in the audio region. At 1 kHz, the effect of eddy-current resistance is negligible.

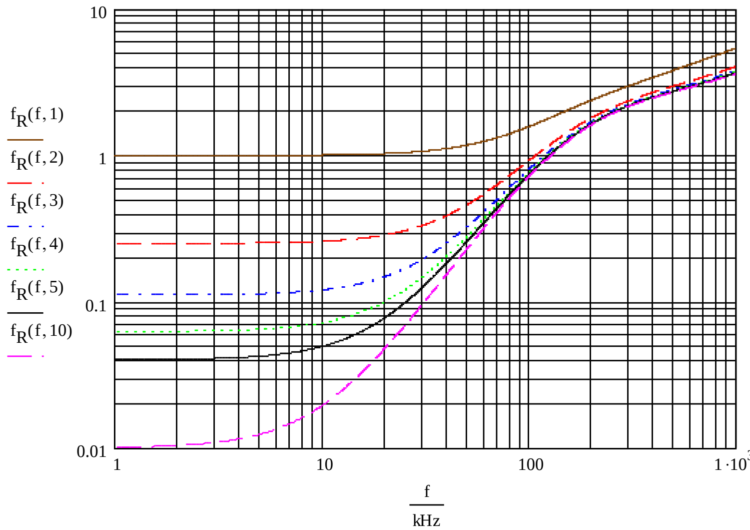

Fig. 8. Log-log plot of constant-strand-size (24 AWG) bundle resistance ratio $f_R(f, M)$ for layers M = 1 through 5 and 10 (N_s = 1 through 25, 100). f_R plots converge at high frequency where M has little effect.

Over the audio range of 20 Hz to 20 kHz, Δf_R as shown in Fig. 9 for 24 AWG wire approaches an asymptotic value with layer or strand counts of slightly over 3.8%. The variation for a single layer (and strand) is somewhat less at 3.1%. With larger wire, the curves retain the same general shape with three distinct regions but shift to lower frequencies as shown in Fig. 10 for a wire size of 20 AWG. An increase in size from 24 AWG to 20 AWG causes a 58% greater increase in Δf_R, of 22.5% at M = 7.

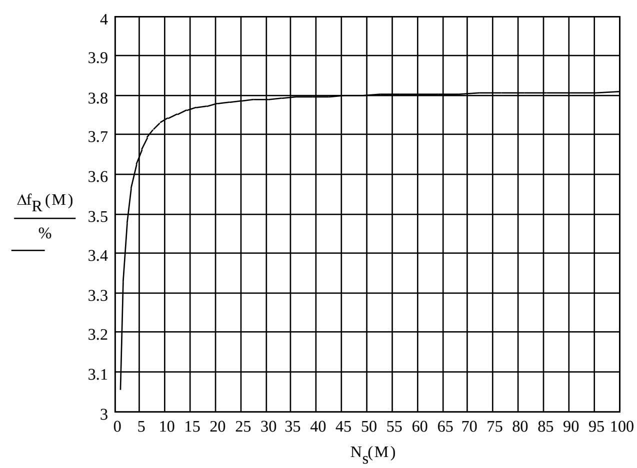

Fig. 9. Graph of $\Delta f_R(M)$ plotted versus $N_s = M^2$ showing a change of 3.06% for a single strand to 3.80% for N_s = 49 (M = 7). Above about 5 layers, the change in Δf_R is negligible for 24 AWG wire.

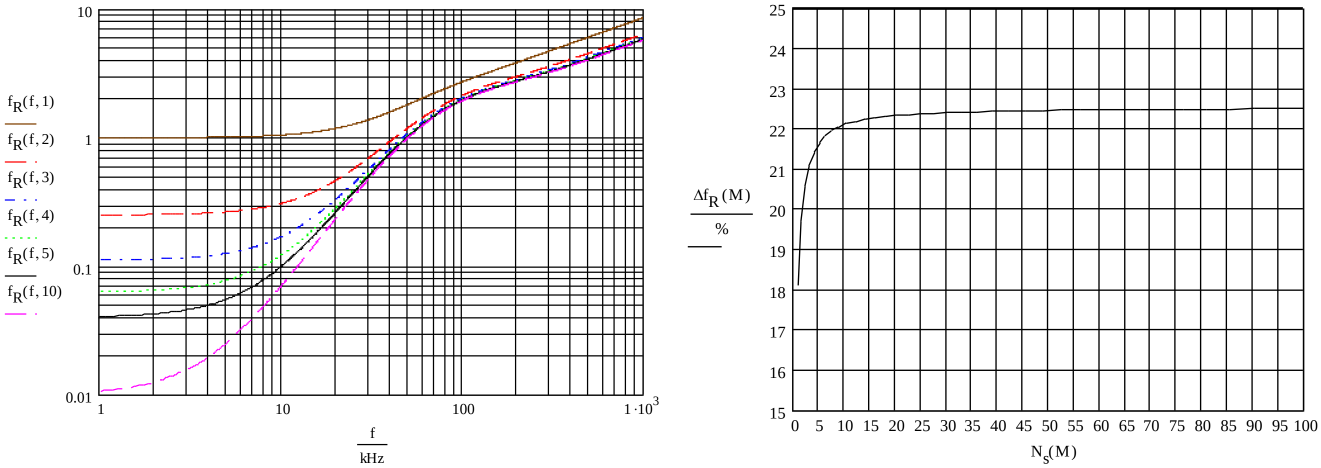

Fig. 10. In these graphs Fig. 8 (left) and Fig. 9 (right) are repeated for larger 20 AWG wire. The f_R curves have shifted to lower frequencies but the change Δf_R is about 22.5% at M = 7 (a big speaker cable), or about 58% higher.

Variation in f_R with frequency causes the frequency response to also vary, but these curves remain constant over time and consequently have a linear low-pass filtering effect. In Fig. 11, wire size is decreased to 28 AWG. The f_R curves predictably shift to the right and Δf_R decreases to 0.61% for 7 layers. A change of wire size has a significant effect on $f_R(f)$. More strands of smaller wire reduce Δf_R, but the benefit is limited by the bundle skin effect whereby the layers have a skin-effect distribution of current in them.

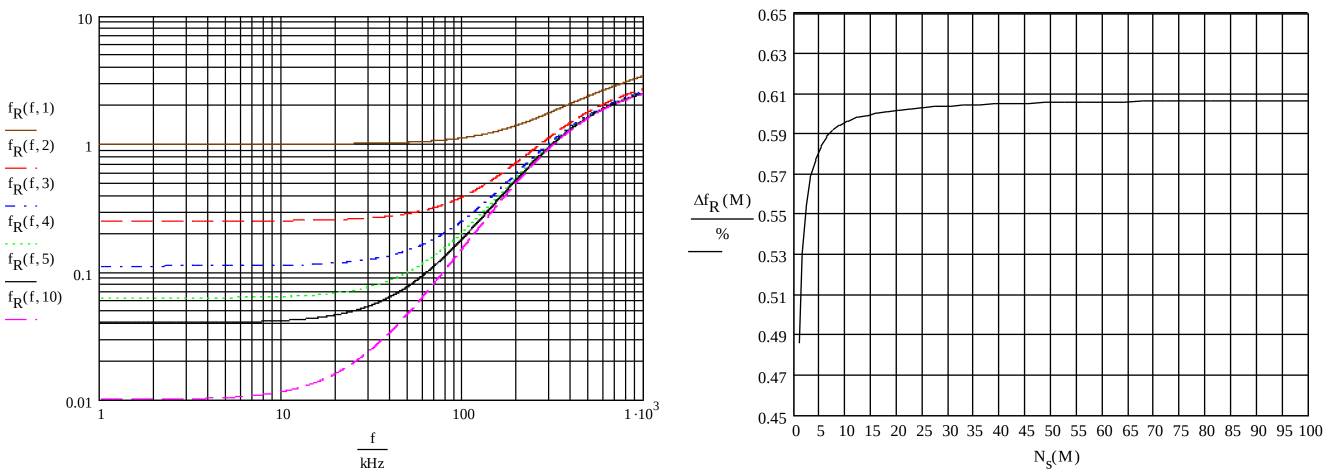

Fig. 11. In these graphs Fig. 10 is repeated with smaller 28 AWG wire. Δf_R now reaches a maximum of about 0.61% for 50 strands, and 0.49% for one strand.

Resistance Variation And Nonlinearity

The effect of varying cable resistance can be analyzed from the circuit in Fig. 12.

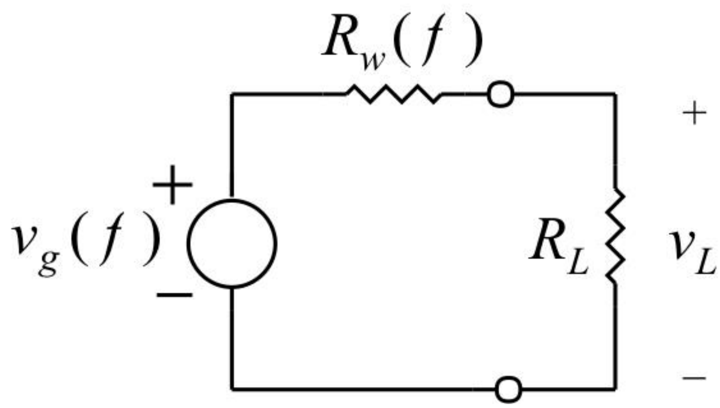

Fig. 12. The equivalent circuit of an amplifier source v_g driving an audio cable of resistance $R_w(f)$ to speaker load resistance R_L. As v_g varies its output frequency, R_w changes with it.

The transmittance of the cable is that of the voltage-divider equation,

$$A_v(f) = \frac{v_L}{v_g(f)} = \frac{R_L}{R_w(f) + R_L} = \frac{1}{1 + \dfrac{R_w(f)}{R_L}}$$

R_w is proportional to f_R. Variation in R_w with frequency varies A_v and results in a modification of the audio-system frequency response. This variation can be frequency-corrected for a constant (flat) response, though $R_w(f)$ is not linear and, like delay lines, does not have a finite number of poles or zeros. It can only be approximately corrected, and this lack of flatness might be what some "golden ears" detect.

The extent of $\Delta A_v(f)$ can be calculated for various audio systems from the foregoing eddy-current formulas. The values for Δf_R over the audio range suggest possible detection in listening tests.

The other identifiable cause of cable resistance variation is self-heating or *thermal distortion* of the cable. Copper has a temperature coefficient (TC) of about 0.4%/°C. A 100-mΩ speaker cable (50 mΩ per conductor, 2 conductors) delivering 5 A to an 8 Ω speaker dissipates 2.5 W. If the cable thermal resistance is 4°C/W, then cable temperature varies with current by 10°C, and $\Delta R_w / R_w$ is about 4%. The fractional change in attenuation to change in R_w before heating is

$$\frac{dA_v / A_v}{dR_w / R_w} = \frac{R_w}{A_v} \cdot \frac{dA_v}{dR_w} = \frac{1}{1 + \dfrac{R_L}{R_w}} = \frac{1}{1 + \dfrac{8\,\Omega}{0.1\,\Omega}} = \frac{1}{81}$$

Thus a 4% change in R_w causes a fractional change in A_v of 4%/81 ≈ 0.05%. Furthermore, this change occurs at thermal rates which can be within the audio spectrum as thermal distortion or "power thermals". The heat-flow rate depends on the *thermal diffusivity* of wire, insulation, and air, though the change in temperature at the heat source within the wire—and hence its resistance—occurs at rates that can be within the audio spectrum.

Assessment

The question of interest is whether thermal or eddy-current effects cause significant intermodulation distortion (IMD) or harmonic distortion (HD). The effect of a varying attenuation $A_v(f)$ with frequency of a linear filter is not distorting because resistance remains constant with frequency. Cable resistance that changes during a frequency sweep causes the circuit to be *time-variant* and hence nonlinear.

Eddy-current effects will cause roll-off of $A_v(f)$ but it will not have the same frequency response as a single-pole RC integrator. Eddy-current variation in cable resistance is reduced by silver- or gold-plating the conductor(s) but will not eliminate distortion from eddy-currents. Even so, plating reduces $\Delta R_w(f)$. Furthermore, eddy currents also cause cable inductance to vary with frequency, and that effect was not included in this introduction to the problem, though it is less likely to be as significant.

Thermal distortion is also a prospective cause of audio distortion but is harder to analyze because thermal diffusivity α is the key variable, and $\alpha(f)$ is hard to measure. Diffusivity is itself a dynamic parameter and for it to vary also causes thermal system time-variance in R_w.

The tentative conclusion is that both cable thermals and eddy currents might cause the distortion that "golden ear" audiophiles claim to hear caused by the cables. Whether these effects are too small to hear is a question requiring nonlinear, time-variant thermal and electric-circuit analysis. Such analysis goes beyond the scope of this article, but it is within the capability of nonlinear systems and control theory to determine the magnitude of the distorting effects by combining thermal and magnetic-field FEA. This is a task for applied mathematicians of the Audio Engineering Society and is on the esoteric fringe ("fringineering") for power electronics!

References

1. "Eddy-Current Effects In Magnetic Design," a six-part series by Dennis Feucht, How2Power Today. See part 6, which contains links to all six articles in the series.
2. *Power Magnetics Design Optimization*, D. Feucht, Innovatia.

About The Author

Dennis Feucht has been involved in power electronics for 40 years, designing motor-drives and power converters. He has an instrument background from Tektronix, where he designed test and measurement equipment and did research in Tek Labs. He has lately been working on projects in theoretical magnetics and power converter research.

For more on magnetics design, see these How2Power Design Guide search results.